Biochimica et Biophysica Acta 1838 (2014) 1382–1388

Contents lists available at ScienceDirect

Biochimica et Biophysica Acta

journal homepage: www.elsevier.com/locate/bbamem

Cell-free synthesis of membrane proteins: Tailored cell models out of microsomes ☆

Susanne F. Fenz [a,1,2], Rita Sachse [b,1], Thomas Schmidt [a], Stefan Kubick [b,*]

[a] Leiden Institute of Physics, Leiden University, PO Box 9504, 2300 RA Leiden, The Netherlands
[b] Fraunhofer IBMT, Branch Potsdam-Golm, Group of Cell-free Protein Synthesis, Am Mühlenberg 13, 14476 Potsdam, Germany

ARTICLE INFO

Article history:
Received 6 September 2013
Received in revised form 27 November 2013
Accepted 16 December 2013
Available online 25 December 2013

Keywords:
Cell-free protein expression
Electroswelling
Membrane protein
Synthetic biology
Vesicle

ABSTRACT

Incorporation of proteins in biomimetic giant unilamellar vesicles (GUVs) is one of the hallmarks towards cell models in which we strive to obtain a better mechanistic understanding of the manifold cellular processes. The reconstruction of transmembrane proteins, like receptors or channels, into GUVs is a special challenge. This procedure is essential to make these proteins accessible to further functional investigation. Here we describe a strategy combining two approaches: cell-free eukaryotic protein expression for protein integration and GUV formation to prepare biomimetic cell models. The cell-free protein expression system in this study is based on insect lysates, which provide endoplasmic reticulum derived vesicles named microsomes. It enables signal-induced translocation and posttranslational modification of *de novo* synthesized membrane proteins. Combining these microsomes with synthetic lipids within the electroswelling process allowed for the rapid generation of giant proteo-liposomes of up to 50 μm in diameter. We incorporated various fluorescent protein-labeled membrane proteins into GUVs (the prenylated membrane anchor CAAX, the heparin-binding epithelial growth factor like factor Hb-EGF, the endothelin receptor ETB, the chemokine receptor CXCR4) and thus presented insect microsomes as functional modules for proteo-GUV formation. Single-molecule fluorescence microscopy was applied to detect and further characterize the proteins in the GUV membrane. To extend the options in the tailoring cell models toolbox, we synthesized two different membrane proteins sequentially in the same microsome. Additionally, we introduced biotinylated lipids to specifically immobilize proteo-GUVs on streptavidin-coated surfaces. We envision this achievement as an important first step toward systematic protein studies on technical surfaces.

1. Introduction

Cells are complex entities with a large variety of active and passive components that serve tasks from defining the structural integrity of the cell to the emergence of cell decision-making through complex and intertwined signaling pathways. As of the sheer complexity our knowledge about the detailed functioning of a cell is still at its infancy. Following Feynman's challenge of "what I cannot create, I do not understand" [1] the construction of cellular functionality into an artificial system is a major challenge that will supposedly lead us to the learned understanding of cellular behavior. In this endeavor well-controlled experiments on biomimetic systems are the essential steps towards a mechanistic understanding of cellular function (for reviews see [2–5]).

One of the simplest cell models, a giant unilamellar vesicle (GUV), consists only of a spherical lipid bilayer enclosing an aqueous buffer that has a size of up to several tens of micrometers in diameter. While GUVs already extensively served as biomimetic models to study lipid-based membrane processes [5], a whole new set of cellular functionality will become accessible upon introduction of functional proteins that are part of cell-signaling pathways into this well-characterized model system. Here, we

Abbreviations: GUVs, Giant unilamellar vesicles; GPCR, G protein-coupled receptor; eYFP, Enhanced yellow fluorescent protein; ETB, Endothelin B receptor; CXCR4, C-X-C chemokine receptor type 4; Hb-EGF, Pro-Heparin-binding epithelial growth factor like factor; ER, Endoplasmic reticulum; E-PCR, Expression polymerase chain reaction; TCA, Trichloroacetic acid; TMD, Transmembrane domain; DOPC, 1,2-dioleoyl-sn-glycero-3-phosphocholine; ITO, Indium tin oxide; DOPE biotin, 1,2-dioleoyl-sn-glycero-3-phosphoethanolamine-N-(cap biotinyl); msd, Mean squared-displacement; *D*, Diffusion coefficient; *E. coli*, *Escherichia coli*; exp., Experimental value; theo., Theoretical value; CFP, Cyan fluorescent protein; PDMS, Polydimethylsiloxane; δ, One-dimensional localization precision; D, Diffusion coefficient; n, Number of integrated target membrane proteins; N, Number of single molecules detected per movie; μ′, Medium's viscosity; μ, Membrane's viscosity; k_B, Boltzmann's constant; T, Temperature; b, mobility; h, Membrane thickness; ε, Reduced radius

☆ Funding sources: This research is supported by the German Ministry of Education and Research (BMBF Nos. 0312039 and 0315942).

* Corresponding author.
E-mail address: Stefan.Kubick@ibmt.fraunhofer.de (S. Kubick).
[1] S. F. Fenz and R. Sachse contributed equally to this work.
[2] Present Addresses: Department of Cell and Developmental Biology, Biocenter, University of Würzburg, Am Hubland, 97074 Würzburg, Germany.

http://dx.doi.org/10.1016/j.bbamem.2013.12.009

concentrate on controlled incorporation of various membrane-anchored and transmembrane proteins with an emphasis on G protein-coupled receptors (GPCRs). GPCRs are membrane proteins of interest for both academia and the pharmaceutical industry as primary drug targets.

A protocol to produce pure lipid GUVs in sucrose solution has been introduced in 1986 [6] and has become a standard preparation technique since. Incorporation of transmembrane proteins into GUVs however is non-trivial and requires specialized protocols that vary for each protein. Early attempts to address a more ubiquitous approach include detergent assisted protein insertion in the membrane of large liposomes [7] in combination with fusogenic peptides [8], and the electroswelling of preformed large proteo-liposomes [9,10]. Only recently, cell-free protein expression systems based on *Escherichia coli* (*E. coli*) were used to prepare small proteo-liposomes that spontaneously fuse with giant liposomes to achieve giant proteo-liposomes [11]. More research on the combination of both techniques, GUV preparation and cell-free protein synthesis, so far focused on the role of vesicles as reaction containers to encapsulate the protein synthesis machinery in synthetic lipid or polymer membranes [12–14]. However, such *E. coli*-based *in vitro* systems do not permit to produce mammalian proteins that include posttranslational modifications like glycosylation without e.g. the addition of exogenous enzymes to reengineer glycosylation pathways [15].

In recent years manifold pro- and eukaryotic *in vitro* expression systems have been established providing the opportunity of well-defined protein synthesis in a viable cell-independent manner. With these cell-free techniques, the expression of a variety of cytotoxic [16,17] as well as membrane spanning proteins (amongst others [18–22]/reviewed in [23]) can be performed within a short time in a versatile fashion. In comparison to the common eukaryotic rabbit reticulocyte lysate supplemented with canine pancreatic microsomal membranes, the insect cell-free system used here provides endogenous microsomes. These are endoplasmic reticulum (ER) derived vesicular structures, enabling the co-translational translocation of membrane proteins into the biological membrane [24–26] in a well-oriented fashion. Furthermore, the methodology allows for posttranslational modification such as glycosylation [22] and lipid modification [27]. Compared to common methods of membrane protein integration into synthetic membranes or micelles, this method does not require any detergent solubilization step.

Here we present the insect based cell-free system and its endogenous microsomes in combination with a tailored GUV formation process as flexible tools for the expression of a variety of membrane proteins in a biological environment. Thus, we are able to build advanced model cells that become accessible to quantitative biophysical interrogation such as single-molecule microscopy.

2. Material and methods

2.1. DNA templates

Expression of the target protein Pro-Heparin-binding epithelial growth factor like factor fused to an enhanced yellow fluorescent protein (Hb-EGF-eYFP) was performed using a pIX3.0 based plasmid template, whereas C-X-C chemokine receptor type 4 (CXCR4-eYFP) and cyan fluorescent protein fused to a CaaX sequence (CFP-CaaX) were synthesized via pcDNA3-vectors. The endogenous signal sequence of Hb-EGF-eYFP was substituted by the Melittin signal sequence (for DNA and peptide sequence see [28]).

The linear expression polymerase chain reaction (E-PCR) product of Endothelin B receptor (ETB) was fused to an eYFP encoding gene sequence. Regulatory sequences obligatory for cell-free expression were added to the gene using three consecutive PCR reactions. First an overlapping sequence for the eYFP fusion was added at the 3′ end of the ETB-encoding sequence and the 5′ complementary sequence for the addition of the regulatory sequences was introduced. In the second PCR step, ETB was fused to the eYFP sequence and the sequence for the addition of 3′ regulatory sequences was introduced. Finally, the E-PCR product was completed in a third amplification reaction by the addition of the final 5′ and 3′ regulatory sequences. PCR primers containing the gene specific and regulatory sequences are listed in Table S1. The PCR reactions were performed using High-Fidelity polymerase and appropriate puffer components from New England Biolabs according to the manufacturer's instructions.

Linear PCR products and circular plasmid cDNA templates were suitable for direct transcription and translation reactions.

2.2. Cell-free protein synthesis

Protein expression was performed in a linked transcription/translation system [28]. Transcription reaction mixes contained 60 μg/mL plasmid DNA or 8 μg/mL E-PCR product, respectively. Transcription was performed for 2 h at 37 °C in case of Hb-EGF-eYFP and for 12 h in case of CXCR4-eYFP and ETB-eYFP. Transcription reaction components were purchased from Qiagen (EasyXpress Insect Kit II). The generated mRNA was purified using DyeEx spin columns (Qiagen) according to the manufacturer's protocol. Lysates generated from *Spodoptera frugiperda* (*Sf*21) cells were used for cell-free protein synthesis in a batch-based mode. Standard lysate preparation was performed as published previously [29]. The gentle disruption of the cells during this procedure leads to the rearrangement of endogenous membranous structures as the ER and their reconstitution as small vesicular structures, called microsomes. The translation reaction contained 25% (v/v) lysate, approximately 250 μg/mL protein encoding mRNA, canonical amino acids (200 mM), ATP (1.75 mM) and GTP (0.45 mM). Reaction mixes for radioactive labeling contained additionally ^{14}C leucine with a final specific radioactivity of 46.2 dpm/pmol. Each protein of interest was expressed separately for 90 min at 27 °C and analyzed as described in the following passage. Fluorescent proteins for microscopic investigations were prepared in the absence of radiolabeled amino acids.

The synthesis of two different types of proteins was performed in a sequential manner. After the initial translation of the first membrane protein, the reaction mixture was separated into vesicular and supernatant fraction by centrifugation (16,000 ×g, 4 °C, 10 min). The vesicular fraction contained the co-translationally translocated protein. The second translation step was prepared by resuspending the vesicular fraction from the initial translation reaction in a vesicle depleted translation reaction mix. Protein synthesis was completed using mRNA coding for the second membrane protein of interest. The translation reaction was performed using standard conditions as previously described.

2.3. Protein separation and autoradiography

Membrane proteins were separated according to their molecular mass using a Nu-PAGE SDS-PAGE system purchased from Life Technologies. 5 μL aliquots of standard translation mixes were acetone precipitated at 4 °C and precipitates were centrifuged at 20,000 ×g for 10 min Protein containing pellets were resuspended in 20 μL of 1× SDS sample buffer. Subsequently samples were separated electro-phoretically using 10% Bis-Tris gels for 35 min at 200 V. Bis-Tris gels were dried for 60 min at 70 °C (Unigeldryer 3545D, Uniequip) and ^{14}C leucine labeled membrane proteins were visualized using the phosphor imaging technique (Typhoon Trio+, Image Eraser, storage phosphor screens and cassettes, ImageQuant TL software, GE Healthcare).

2.4. Quantification of de novo synthesized membrane proteins

Protein yield was determined using hot trichloroacetic acid (TCA) precipitation and scintillation quantification. 3 mL of a 10% (v/v) TCA solution containing 2% (w/v) casein hydrolysate were added to 5 μL of the translation reaction mix containing ^{14}C leucine labeled membrane proteins. The translation mix was heated for 15 min at 80 °C followed by subsequent cooling for 30 min at 4 °C. The precipitated proteins

were separated and dried by filtration (filtration paper MN GF-3, Macherey-Nagel). Filters were washed twice with 5% (v/v) TCA and acetone. Proteins retained on the filter membrane were incubated with a scintillation cocktail (Quicksafe A, Zinsser Analytic) for 1 h. In case of ^{14}C leucine labeled protein, the scintillation sample was analyzed with the LS6500 scintillation counter (Beckman Coulter).

2.5. Electroswelling

Giant proteo-liposomes were swollen from target protein harboring microsomes obtained from cell-free protein expression combined with synthetic lipids. For that purpose, 1 μL of DOPC (1,2-dioleoyl-sn-glycero-3-phosphocholine, Avanti Polar Lipids, USA) dissolved in chloroform (2 mg/mL) was deposited on an ITO (indium tin oxide, Diamond Coatings, UK) coated glass slide (25.8 mm × 25.8 mm × 0.2 mm) and dried under vacuum for several hours. Subsequently, 1 μL of the microsome mixture was added and partially dried under flow of nitrogen. A slice of PDMS (Polydimethylsiloxane) (Sylgard 184, 1:10, Dow Corning) with a hole in the center, supported by the first ITO glass, served as a distance element forming the swelling chamber that was filled with PBS (Gibco) or PBS supplemented with 200 mOsM/L sucrose (Life Technologies). The chamber was closed with another ITO glass slide and each ITO glass was connected to the function generator (Hameg, Germany) via a copper wire attached to the glass with the help of copper tape. In a typical experiment a voltage of 4 V was applied at 500 Hz for 10 h. A sketch of the experimental setup is depicted in SI Fig. S1.

2.6. Immobilization assay

The employed immobilization assay was based on the well-established biotin–avidin interaction that is routinely being used for liposome targeting since the 1980th [30]. The DOPC mix mentioned in the electroswelling experiment (Section 2.5) was supplemented with 10 mol% DOPE-biotin (1,2-dioleoyl-sn-glycero-3-phospho-ethanolamine-N-(cap biotinyl), Avanti Polar Lipids) to produce GUVs for the immobilization assay. GUVs were swollen in the presence of PBS plus 200 mOsM/L sucrose and transferred to the glass-bottom observation chamber filled with PBS plus 200 mOsM/L glucose (Life Technologies). The glass was previously functionalized by incubation with 75 μM BSA-biotin (Sigma) for 15 min and subsequent binding of 1 μM streptavidin (Sigma) for 30 min Incubations were terminated by washing with PBS. After the last washing step, PBS was exchanged for PBS plus 200 mOsM/L glucose.

2.7. Single-molecule microscopy

The experimental setup for wide-field single-molecule imaging has been described in detail previously [31]. In brief, the samples were mounted onto an inverted microscope (Axiovert100, Zeiss, Germany), equipped with a high-numerical aperture oil objective (Plan-Apochromat, 100×, NA = 1.4, Zeiss, Germany) and a filter-set suitable for eYFP (dichroic Z405/514/647/1064rpc, emission Z514/647 m Chroma, USA). An argon-ion laser (Spectra Physics, USA) was used in combination with an acusto-optical-tunable filter (AA Opto-Electronics, France) to illuminate the sample at 514 nm and 2 kW/cm^2 for 5 ms per frame. Movies of typically 1500 frames were recorded at 20 Hz on a liquid nitrogen cooled camera (Princeton Instruments, USA). The region-of-interest was set to 50 × 50 pixels. The apparent pixel-size was 202 nm.

For the two-color experiment (Fig. 4), we additionally used 405 nm (Crysta laser, USA) to excite CFP fluorescence at 1.5 kW/cm^2 for 5 ms and replaced the dichroic by ZT458/514/594rpc (Chroma, USA). The blue (CFP) and yellow (YFP) channel were recorded sequentially to prevent potential crosstalk.

2.8. Single-molecule localization and tracking

In order to accurately localize the molecules of interest throughout a recorded single-molecule movie, image processing was indispensable. Details on background subtraction and noise treatment are published elsewhere [5]. Each detected diffraction-limited spot was fitted with a two-dimensional Gaussian function to localize the molecules of interest with a precision of 35 nm. The obtained single-molecule positions were the starting point for single-particle tracking. The necessary steps to generate trajectories have been described in detail in [5]. In brief, a probabilistic algorithm is used to connect the positions of molecules in two frames of a movie (frames *i* and *j*). A transitional matrix was built up which includes the probabilities of all possible connections between all molecules in frames *i* and *j*. Trajectories were constructed by optimizing for the combination of all connections with the highest total probability. We calculated the resulting mean squared-displacement (msd) as a function of the time lag between the individual frames and subtracted the offset originating from the limited localization precision as determined from the Gaussian fit: $offset = msd(t = 0) = 4\delta^2$, where δ denotes the one-dimensional localization precision. The corrected data was fitted with a one-dimensional diffusion model to determine the molecule's diffusion coefficient D in the GUV membrane: $msd_{corr} = 2Dt$.

3. Results

Synthetic lipids (DOPC) were deposited on conducting ITO glass below insect-based cell-free derived microsomes. In comparison to earlier work on GUV preparation from pure microsomes [27], incorporation of synthetic lipids greatly facilitated microsomal vesicle fusion during electroswelling (from 30 h [27] down to 5 h; see Fig. 1).

Furthermore, the introduction of synthetic lipids allowed us to provide GUVs with additional functionality. E.g. we added lipids with a biotinylated headgroup to achieve 'sticky' GUVs, that can be specifically immobilized to designated loci, a requirement for any lab-on-a-chip screening application. The strength of the immobilization was assayed by hydrodynamic flow. As seen in SI Fig. S2 the vesicle was disturbed by the hydrodynamic stress, whereas the basal part of the membrane stayed in contact with the support ensuring that the GUV returned to its initial position once the flow was removed.

We focused on the combination of cell-free protein synthesis to incorporate the membrane protein of interest into the biological membrane and GUV formation for vesicle enlargement while supporting the membrane swelling with synthetic lipids. Starting from either plasmid DNA or a linear PCR product, we successfully produced GUVs containing various fluorescent protein-labeled membrane proteins: the membrane

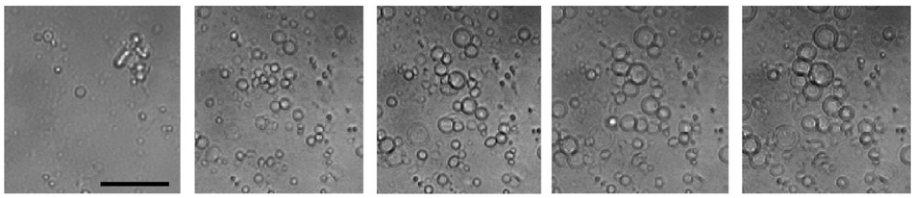

Fig. 1. Time lapse microscopy of lipid-assisted GUV electroswelling from insect cell-free system based microsomes. Scale bar 75 μm.

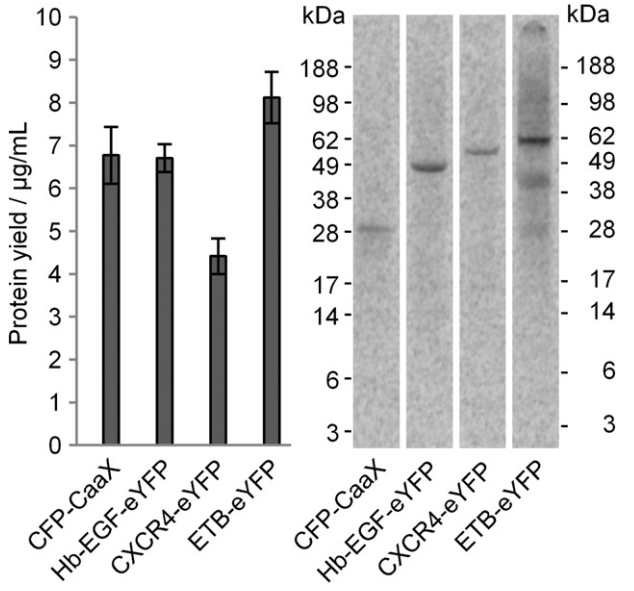

Fig. 2. Qualitative and quantitative analysis of ^{14}C-labled cell-free expressed membrane proteins CFP-CaaX, Hb-EGF-eYFP, CXCR4-eYFP and ETB-eYFP. (a) Quantification of total protein yields generated within a cell-free protein synthesis reaction, (b) autoradiograph of target proteins separated by their molecular mass.

anchored YFP-CaaX [27], the Pro-Heparin-binding epithelial growth factor like factor (Hb-EGF-eYFP) harboring a single transmembrane domain (1 TMD) and two examples of G-protein coupled receptors exhibiting seven transmembrane domains: (7 TMD) the Endothelin B receptor (ETB-eYFP) and the C-X-C chemokine receptor type 4 (CXCR4-eYFP). For that purpose, we pre-synthesized the membrane protein into the microsomes and used the microsomes as target protein harboring modules for the GUV swelling process. To assess the efficiency of the cell-free expression method we performed radiolabeling of the *de novo* synthesized protein in the crude translation reaction mixture. We complemented these results by single-molecule imaging of the fluorescently labeled target proteins in the GUV membrane to estimate the final concentration of cell-free synthesized protein in the cell models. The total yields of the *de novo* cell-free protein synthesis were in the range of 4–8 µg/mL (Fig. 2(a)) and the autoradiograph of the molecular mass separated membrane proteins showed distinct bands at the expected molecular masses (see Fig. 2(b)). Side products of smaller molecular mass, mainly observed in the ETB expression reaction may have been result of partial expression or degradation of the full length protein.

As an independent method to assess protein localization, potential dimerization and incorporation into the vesicle bilayer, single-molecule imaging was performed. We focused on the equatorial plane of the GUVs such that proteins in the GUV membrane appeared along the perimeter of a circle as depicted in Fig. 3 for the example of Hb-EGF-eYFP. See SI Fig. S3 for single-molecule snapshots of GUVs exhibiting ETB-eYFP and CXCR4-eYFP. We observed individual, mobile, diffraction limited fluorescence signals that had the characteristics of individual YFP-fusion proteins [32]. Molecules were localized with a precision of 35 nm and the overlay of all positions recovers the outline of the GUV Fig. 3(c).

We recorded movies of $1–8 \cdot 10^4$ individual proteins on 22–50 GUVs to determine the mobility of the single transmembrane Hb-EGF-eYFP as well as the seven transmembrane CXCR4-eYFP and ETB-eYFP in the membrane of giant vesicles, respectively. In agreement with the predicted free-diffusion behavior, the msd increased linearly with the time between observations (see SI Fig. S4).

After correction for the limited localization precision, a linear fit to the data yielded an experimental diffusion constant, $D_{Hb\text{-}EGF,exp.}$, of (3.7 ± 0.2) µm^2/s, $D_{CXCR4,exp.} = D_{ETB,exp.}$, of (2.7 ± 0.1) µm^2/s. This range of diffusion constants were predicted given that the membrane consisted of a mixture of 'natural' ER membrane and synthetic lipids (membrane proteins in synthetic vesicles 1–10 µm^2/s [8,10,33,34], membrane proteins in cell membranes (0.1–0.01) µm^2/s [35–38]).

To determine the amount of target protein in the proteo-GUVs after the electroswelling process, we estimated the number of integrated target membrane proteins, n, from the number, N, of single molecules detected per movie. Taking into consideration the limits of the observation volume (focal plane $\approx$ 1 µm) and the length of a movie (75 s), for an exemplary GUV with r = 5 µm, only 20% of the GUV surface is observed. Individual molecules with D $\approx$ 3 µm^2/s may reappear inside the observation volume on average 3 times. Thus, we conclude n = N/0.6. The estimate is a lower boundary, because during recording single molecule tend to bleach at a higher rate than they recover and sometimes prebleaching of GUV was necessary to allow for single-molecule imaging. We tracked approximately 250 proteins/GUV for the 7 TMD receptors and approximately 850 proteins/GUV for the 1 TMD Hb-EGF-eYFP (Table 1).

In a next step towards more complex systems we combined two different proteins in the same GUV, subsequent to sequential synthesis of each protein into the same set of microsomes. Here, we present data on CFP-CaaX and Hb-EGF-eYFP as an example. Dual channel single-molecule microscopy clearly revealed that both proteins were present simultaneously in the same GUV (Fig. 4).

4. Discussion

A major advantage of our approach to produce giant proteoliposomes from a combination of *in vitro* protein synthesis and electroswelling is its versatility. The methodology can be easily applied to a wide range of structurally and functionally divergent membrane proteins. Presynthesis of the target proteins enables the directed integration of membrane proteins, carrying a signal sequence for the process of co-translational translocation, into the membranes of the ER-based microsomes.

The detailed mobility analysis as presented above was further used to assess the oligomerization state of the receptors in the GUVs. The

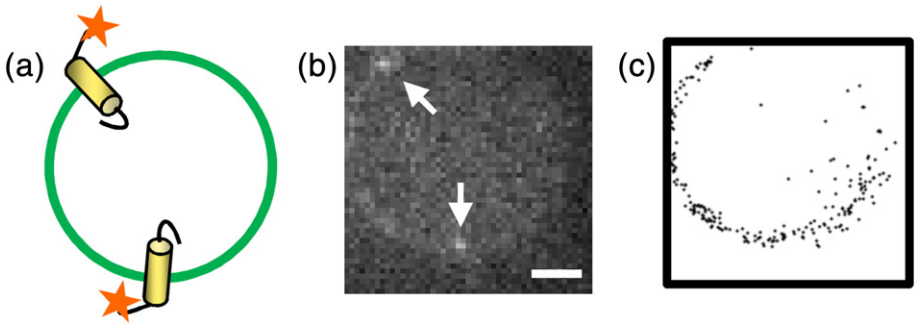

Fig. 3. Single molecule imaging of Hb-EGF-eYFP in the GUV membrane. (a) Sketch. (b) The white arrows highlight two single Hb-EGF-eYFP molecules. (c) Overlay of all single-molecule positions detected during one movie. Scale bar 2 µm. Note that (a) is not to scale.

Table 1
Estimation of the number of cell-free expressed membrane proteins per GUV, n, from the number, N, of single molecules detected per movie. The limiting parameters are observation volume (focal plane ≈ 1 μm) and the length of a movie (75 s). For an exemplary GUV with r = 5 μm, only 20% of the GUV surface was observed, but individual molecules with D ≈ 3 μm²/s may reappear inside the observation volume on average 3 times. Thus n = N/0.6; ± standard deviation.

Protein	N	n
Hb-EGF-eYFP	520 ± 310	850
ETB-eYFP	150 ± 60	250
CXCR4-eYFP	160 ± 90	250

Saffman–Delbrück model [39] gives a relation to calculate the diffusion constant D of a cylinder with radius a in a membrane with viscosity μ surrounded by a medium with viscosity μ′, but it can provide only an asymptotic solution for a certain range of cylinder size and viscosities of the membrane and ambient media [40]:

$$D = k_B T b \quad , \text{ with } \quad b = \frac{1}{4\pi\mu h}\left(\log\frac{\mu h}{\mu' a} - \gamma\right) \tag{1}$$

where k_B denotes the Boltzmann's constant, T the temperature, b the mobility, and h the membrane thickness.

To test whether these conditions are fulfilled in the given experimental setting, we used the argument by Petrov and Schwille [41]:

$$\varepsilon<1 \quad , \text{ with } \quad \varepsilon = \frac{2a\mu'}{\mu h} \tag{2}$$

where ε denotes the reduced radius. ε was calculated for Hb-EGF-eYFP ($a_{Hb\text{-}EGF}$ = 0.6 nm; structural information about the radius of the transmembrane domain of Hb-EGF-eYFP was retrieved by modeling the known amino acid sequence [42] on an α helix using the software Swiss pdb Viewer.) diffusing in a GUV membrane (h = 5 nm) consisting of a mixture of synthetic and natural lipids (μ ≈ 0.1 Pa s), surrounded by an aqueous solution (μ′ = 0.001 Pa s), yielding ε = 0.0024. For this calculation we had to estimate the hybrid membrane viscosity: taking into consideration measurements on various synthetic [43] and life cell membranes [44,45], we assume that μ = 100 μ′, with μ′ = 1 mPa s.

The comparison of the experimentally measured diffusion constant of the single pass transmembrane protein Hb-EGF-eYFP with the theoretical prediction by Saffman and Delbrück (see Eq. (1)) yields $D_{1TMD,theo}$ = 4.0 μm²/s. $D_{Hb\text{-}EGF,exp}$ = 3.7 ± 0.2 μm²/s (see Table 2).

The Saffman–Delbrück model predicts a logarithmic scaling law of the diffusion constant, D, as a function of the transmembrane domain radius, a. Thus, starting from the measured value for Hb-EGF-eYFP ($D_{Hb\text{-}EGF,exp.}$ = 3.7 ± 0.2 μm²/s, $a_{Hb\text{-}EGF}$ = 0.6 nm) the diffusion constant of CXCR4 with seven transmembrane domains (a_{7TMD} = 1.7 nm [46]) can be calculated: $D_{7TMD,theo.}$ = 3.1 μm²/s. The theoretical prediction slightly overestimates the measurements on CXCR4-eYFP: $D_{CXCR4,exp.}$ = 2.7 ± 0.1 μm²/s (Table 2). If we start from the measured diffusion constant and back-calculate the corresponding size of the diffusing object, we get a_{CXCR4} = 3.2 nm. This result indicates that the CXCR4 receptor might appear in a dimeric configuration, as has been reported for various G protein-coupled receptors [47]. This result might also be transferrable to the ETB receptor, although the exact structural data to prove this point are missing.

Comparison of the experimentally measured diffusion constant of the single pass transmembrane protein Hb-EGF-eYFP with the theoretical prediction by Saffman and Delbrück (see Eq. (1)) yields $D_{1TMD,theo.}$ = 4.0 μm²/s and thus good agreement with the experimental result $D_{Hb\text{-}EGF,exp.}$ = 3.7 ± 0.2 μm²/s.

The combination of different membrane proteins into the same set of GUVs opens the opportunity to study interactions between functional pairs of proteins in the near future, e.g. GPCR interactions in a vesicle based cell model.

Table 2
Diffusions constants of transmembrane proteins in GUV membranes. Comparison of experimental (exp.) values and theoretical (theo.) predictions according to the Saffman–Delbrück model; ± standard deviation.

	Hb-EGF exp.	1 TMD theo.	CXCR4 exp.	ETB exp.	7 TMD theo.
D[μm²/s]	3.7 ± 0.2	4.0	2.7 ± 0.1	2.7 ± 0.1	3.1

In general, the fact that the measured protein diffusion constants were closer to the values reported for synthetic membranes indicates that the membrane of the hybrid vesicles presented here comprises mainly of the supplemented synthetic lipid DOPC while the natural ER membrane lipids were negligible. However, the hybrid character of the formed proteo-GUVs consists of cell-free expressed membrane proteins residing in a largely synthetic membrane. With this we were able to establish a flexible and adaptable method for studies of difficult to express membrane proteins on well-defined GUVs.

In this context, the synthesis of active membrane proteins, as GPCRs, is of major interest for future structural and functional studies. An outstanding milestone in this field was the determination of the high-resolution three-dimensional structure of a β-Adrenergic receptor interacting with its ligand. The protein expression for this study was based on an insect cell culture over-expression system [48]. However, the expression of sufficient amounts of such complex membrane proteins in viable cells is still challenging due to cytotoxic effects and protein aggregation. To overcome these problems cell-free expression systems have become an applicable tool for membrane protein expression. Only recently, cell-free protein expression systems based on *E. coli* lysates were combined with synthetic lipids to prepare small proteo-liposomes or nanodiscs harboring different GPCRs, e.g. the ETB receptor. These proteo-liposomes and nanodiscs were used to study protein–ligand interactions [49]. Eukaryotic cell-free protein expression systems in combination with the immobilization of hybrid-GUVs, the method assignment presented in our publication, provide a basis for the reconstitution of complex membrane protein pathways and

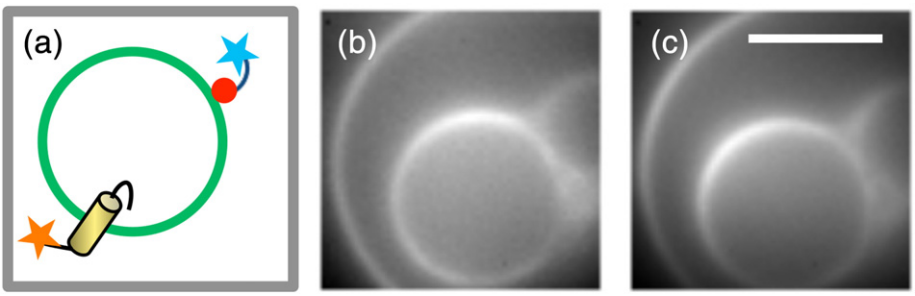

Fig. 4. GUV exhibiting two membrane proteins: CFP-CaaX and Hb-EGF-eYFP. (a) Sketch. (b) CFP channel. (c) YFP channel. The presented fluorescence images are mean images averaged over 1500 frames of a single-molecule movie. The scale bar is 5 μm and valid for (b) and (c). Note that (a) is not to scale.

their study on fixed GUVs in a well-defined and cell independent surrounding.

5. Conclusions

In this study we present a homogeneous insect-based expression system that provides membrane protein yields up to several μg/mL and that permits to construct biological functionality into giant synthetic vesicles. Endogenous insect microsomal vesicles form the basis for directed membrane protein integration as well as posttranslational modification. Within our procedure, the microsomes serve as flexible and adaptable functional modules carrying the membrane proteins of interest. In contrast to fully synthetic GUVs, the hybrid GUVs generated in this study consisted of synthetic lipids as well as microsomal membrane proteins. Thus they are an intermediate between fully synthetic models and biological systems for the study of biophysical problems. Based on the ability of the cell-free system to express versatile types of lipid anchored proteins as well as integral membrane proteins, such as GPCRs, our methodology offers the future perspective to reconstitute entire signal transduction pathways for ligand detection and protein–protein interaction studies that will result in a fundamental mechanistic understanding of membrane–protein interactions and cell regulation.

Acknowledgment

We would like to thank Dr. Nicola Jones, University of Würzburg, for her help on deriving structural information about the Hb-EGF-eYFP helix. Plasmid DNA encoding for Hb-EGF-eYFP and ETB was kindly provided by Prof. Dr. Michael Schaefer (Universität Leipzig).

Appendix A. Supplementary data

Supplementary data to this article can be found online at http://dx.doi.org/10.1016/j.bbamem.2013.12.009.

References

[1] S.R. Feynman, attributed in: Hawking (Ed.), The Universe in a Nutshell, Bantam Books, 2001.
[2] A.S. Smith, Physics challenged by cells, Nat. Phys. 6 (2010) 726–729.
[3] A.P. Liu, D.A. Fletcher, Biology under construction: in vitro reconstitution of cellular function, Nat. Rev. Mol. Cell Biol. 10 (2009) 644–650.
[4] P. Schwille, S. Diez, Synthetic biology of minimal systems, Crit. Rev. Biochem. Mol. Biol. 44 (2009) 223–242.
[5] S.F. Fenz, K. Sengupta, Giant vesicles as cell models, Integr. Biol. 4 (2012) 982–995.
[6] M.I. Angelova, D.S. Dimitrov, Liposome electroformation, Faraday Discuss. Chem. Soc. 81 (1986) 303–311.
[7] J.L. Rigaud, M.T. Paternostre, A. Bluzat, Mechanisms of membrane protein insertion into liposomes during reconstitution procedures involving the use of detergents. 2. Incorporation of the light-driven proton pump bacteriorhodopsin, Biochemistry 27 (1988) 2677–2688.
[8] N. Kahya, E.I. Pecheur, W.P. de Boeij, D.A. Wiersma, D. Hoekstra, Reconstitution of membrane proteins into giant unilamellar vesicles via peptide-induced fusion, Biophys. J. 81 (2001) 1464–1474.
[9] P. Girard, J. Pecreaux, G. Lenoir, P. Falson, J.L. Rigaud, P. Bassereau, A new method for the reconstitution of membrane proteins into giant unilamellar vesicles, Biophys. J. 87 (2004) 419–429.
[10] . M.K. Doeven, J.H. Folgering, V. Krasnikov, E.R. Geertsma, G. van den Bogaart, B. Poolman, Distribution, lateral mobility and function of membrane proteins incorporated into giant unilamellar vesicles, Biophys. J. 88 (2005) 1134–1142.
[11] A. Varnier, F. Kermarrec, I. Blesneac, C. Moreau, L. Liguori, J.L. Lenormand, N. Picollet-D'hahan, A simple method for the reconstitution of membrane proteins into giant unilamellar vesicles, J. Membr. Biol. 233 (2010) 85–92.
[12] S.M. Christensen, D. Stamou, Surface-based lipid vesicle reactor systems: fabrication and applications, Soft Matter 3 (2007) 828–836.
[13] Z. Nourian, W. Roelofsen, C. Danelon, Triggered gene expression in fed-vesicle microreactors with a multifunctional membrane, Angew. Chem. Int. Ed. 51 (2012) 3114–3118.
[14] C. Martino, S.-H. Kim, L. Horsfall, A. Abbaspourrad, S.J. Rosser, J. Cooper, D.A. Weitz, Protein expression, aggregation, and triggered release from polymersomes as artificial cell-like structures, Angew. Chem. Int. Ed. 51 (2012) 6416–6420.
[15] C. Guarino, M.P. DeLisa, A prokaryote-based cell-free translation system that efficiently synthesizes glycoproteins, Glycobiology 22 (2012) 596–601.
[16] J.H. Orth, B. Schorch, S. Boundy, R. Ffrench-Constant, S. Kubick, K. Aktories, Cell-free synthesis and characterization of a novel cytotoxic pierisin-like protein from the cabbage butterfly Pieris rapae, Toxicon 57 (2011) 199–207.
[17] Y. Xun, P. Tremouilhac, C. Carraher, C. Gelhaus, K. Ozawa, G. Otting, N.E. Dixon, M. Leippe, J. Grotzinger, A.J. Dingley, A.V. Kralicek, Cell-free synthesis and combinatorial selective 15 N-labeling of the cytotoxic protein amoebapore A from Entamoeba histolytica, Protein Expr. Purif. 68 (2009) 22–27.
[18] J.J. Wuu, J.R. Swartz, High yield cell-free production of integral membrane proteins without refolding or detergents, Biochim. Biophys. Acta 5 (2008) 11.
[19] C. Klammt, D. Schwarz, K. Fendler, W. Haase, V. Dötsch, F. Bernhard, Evaluation of detergents for the soluble expression of alpha-helical and beta-barrel-type integral membrane proteins by a preparative scale individual cell-free expression system, FEBS J. 272 (23) (2005) 6024–6038.
[20] R. Kalmbach, I. Chizhov, M.C. Schumacher, T. Friedrich, E. Bamberg, M. Engelhard, Functional cell-free synthesis of a seven helix membrane protein: in situ insertion of bacteriorhodopsin into liposomes, J. Mol. Biol. 371 (2007) 639–648.
[21] F. Katzen, J.E. Fletcher, J.P. Yang, D. Kang, T.C. Peterson, J.A. Cappuccio, C.D. Blanchette, T. Sulchek, B.A. Chromy, P.D. Hoeprich, M.A. Coleman, W. Kudlicki, Insertion of membrane proteins into discoidal membranes using a cell-free protein expression approach, J. Proteome Res. 7 (8) (2008) 3535–3542.
[22] R. Sachse, D. Wüstenhagen, M. Šamalíková, M. Gerrits, F.F. Bier, S. Kubick, Synthesis of membrane proteins in eukaryotic cell-free systems, Eng. Life Sci. 13 (2013) 39–48.
[23] F. Katzen, T.C. Peterson, W. Kudlicki, Membrane protein expression: no cells required, Trends Biotechnol. 27 (8) (2009) 455–460.
[24] G. Blobel, B. Dobberstein, Transfer of proteins across membranes. I. Presence of proteolytically processed and unprocessed nascent immunoglobulin light chains on membrane-bound ribosomes of murine myeloma, J. Cell Biol. 67 (1975) 835–851.
[25] D. Gorlich, T.A. Rapoport, Protein translocation into proteoliposomes reconstituted from purified components of the endoplasmic reticulum membrane, Cell 75 (1993) 615–630.
[26] S. Pfeffer, F. Brandt, T. Hrabe, S. Lang, M. Eibauer, R. Zimmermann, F. Forster, Structure and 3D arrangement of endoplasmic reticulum membrane-associated ribosomes, Structure 20 (2012) 1508–1518.
[27] P.M. Shaklee, S. Semrau, M. Malkus, S. Kubick, M. Dogterom, T. Schmidt, Protein incorporation in giant lipid vesicles under physiological conditions, Chembiochem 11 (2) (2010) 175–179.
[28] S. Kubick, M. Gerrits, H. Merk, W. Stiege, V.A. Erdmann, In vitro synthesis of posttranslationally modified membrane proteins, "Membrane Protein Crystallization" Current Topics in Membranes, Elsevier, 2009, (Chapter 2).
[29] M. Stech, H. Merk, J.A. Schenk, W.F. Stöcklein, D.A. Wüstenhagen, B. Micheel, C. Duschl, F.F. Bier, S. Kubick, Production of functional antibody fragments in a vesicle-based eukaryotic cell-free translation system, J. Biotechnol. 164 (2) (2012) 220–231.
[30] B. Rivnay, E.A. Bayer, M. Wilchek, Use of avidin-biotin technology for liposome targeting, Methods Enzymol. 149 (1987) 119–123.
[31] T. Schmidt, G.J. Schutz, W. Baumgartner, H.J. Gruber, H. Schindler, Imaging of single molecule diffusion, Proc. Natl. Acad. Sci. U. S. A. 93 (1996) 2926–2929.
[32] G.S. Harms, L. Cognet, P.H. Lommerse, G.A. Blab, T. Schmidt, Autofluorescent proteins in single-molecule research: applications to live cell imaging microscopy, Biophys. J. 80 (2001) 2396–2408.
[33] T. Ohtsuka, S. Neki, T. Kanai, K. Akiyoshi, S.M. Nomura, T. Ohtsuki, Synthesis and in situ insertion of a site-specific fluorescently labeled membrane protein into cell-sized liposomes, Anal. Biochem. 418 (2011) 97–101.
[34] J. Kriegsmann, I. Gregor, I. von der Hocht, J. Klare, M. Engelhard, J. Enderlein, J. Fitter, Translational diffusion and interaction of a photoreceptor and its cognate transducer observed in giant unilamellar vesicles by using dual-focus FCS, Chembiochem 10 (2009) 1823–1829.
[35] K. Ahlen, P. Ring, B. Tomasini-Johansson, K. Holmqvist, K.E. Magnusson, K. Rubin, Platelet-derived growth factor-BB modulates membrane mobility of beta1 integrins, Biochem. Biophys. Res. Commun. 314 (2004) 89–96.
[36] D. Axelrod, P. Ravdin, D.E. Koppel, J. Schlessinger, W.W. Webb, E.L. Elson, T.R. Podleski, Lateral motion of fluorescently labeled acetylcholine receptors in membranes of developing muscle fibers, Proc. Natl. Acad. Sci. U. S. A. 73 (1976) 4594–4598.
[37] D.E. Golan, C.S. Brown, C.M. Cianci, S.T. Furlong, J.P. Caulfield, Schistosomula of Schistosoma mansoni use lysophosphatidylcholine to lyse adherent human red blood cells and immobilize red cell membrane components, J. Cell Biol. 103 (1986) 819–828.
[38] E.D. Sheets, G.M. Lee, R. Simson, K. Jacobson, Transient confinement of a glycosylphosphatidylinositol-anchored protein in the plasma membrane, Biochemistry 36 (1997) 12449–12458.
[39] P.G. Saffman, M. Delbruck, Brownian motion in biological membranes, Proc. Natl. Acad. Sci. U. S. A. 72 (1975) 3111–3113.
[40] B.D. Hughes, B.A. Pailthorpe, L.R. White, The translational and rotational drag on a cylinder moving in a membrane, J. Fluid Mech. 110 (1981) 349–372.
[41] E.P. Petrov, P. Schwille, Translational diffusion in lipid membranes beyond the Saffman–Delbruck approximation, Biophys. J. 94 (5) (2008) L41–L43(Erratum in, Biophys J. 2012 Jul 2018;2103(2012):2375.).
[42] J.A. Abraham, D. Damm, A. Bajardi, J. Miller, M. Klagsbrun, R.A. Ezekowitz, Heparin-binding EGF-like growth factor: characterization of rat and mouse

cDNA clones, protein domain conservation across species, and transcript expression in tissues, Biochem. Biophys. Res. Commun. 190 (1993) 125–133.
[43] C.E. Kung, J.K. Reed, Fluorescent molecular rotors: a new class of probes for tubulin structure and assembly, Biochemistry 28 (1989) 6678–6686.
[44] W.R. Dunham, R.H. Sands, S.B. Klein, E.A. Duell, L.M. Rhodes, C.L. Marcelo, EPR measurements showing that plasma membrane viscosity can vary from 30 to 100 cP in human epidermal cell strains, Spectrochim. Acta A Mol. Biomol. Spectrosc. 52 (1996) 1357–1368.
[45] J. Kapitulnik, E. Weil, R. Rabinowitz, M.M. Krausz, Fetal and adult human liver differ markedly in the fluidity and lipid composition of their microsomal membranes, Hepatology 7 (1987) 55–60.
[46] B. Wu, E.Y. Chien, C.D. Mol, G. Fenalti, W. Liu, V. Katritch, R. Abagyan, A. Brooun, P. Wells, F.C. Bi, D.J. Hamel, P. Kuhn, T.M. Handel, V. Cherezov, R.C. Stevens, Structures of the CXCR4 chemokine GPCR with small-molecule and cyclic peptide antagonists, Science 330 (2010) 1066–1071.
[47] S. Angers, A. Salahpour, M. Bouvier, Dimerization: an emerging concept for G protein-coupled receptor ontogeny and function, Annu. Rev. Pharmacol. Toxicol. 42 (2002) 409–435.
[48] S.G. Rasmussen, B.T. DeVree, Y. Zou, A.C. Kruse, K.Y. Chung, T.S. Kobilka, F.S. Thian, P.S. Chae, E. Pardon, D. Calinski, J.M. Mathiesen, S.T. Shah, J.A. Lyons, M. Caffrey, S.H. Gellman, J. Steyaert, G. Skiniotis, W.I. Weis, R.K. Sunahara, B.K. Kobilka, Crystal structure of the beta2 adrenergic receptor-Gs protein complex, Nature 477 (2011) 549–555.
[49] D. Proverbio, C. Roos, M. Beyermann, E. Orbán, V. Dötsch, F. Bernhard, Functional properties of cell-free expressed human endothelin A and endothelin B receptors in artificial membrane environments, Biochim. Biophys. Acta Biomembr. 1828 (2013) 2182–2192.